

Phytogetic aqueous extract mediated fabrication of Ag-Fe₂O₃ nanohybrids for detoxification of carcinogenic Congo Red dye: An Environmental Remediation approach

Faraz Ahmed¹, Tahsin Gulzar^{1*}, Tahseen Kamal², Shumaila Kiran¹ and Ikram Ahmad³

¹Department of Applied Chemistry, Govt. College University Faisalabad-38000, Punjab Pakistan

²Center of Excellence for Advanced Materials Research, King Abdulaziz University, Jeddah 21589, Saudi Arabia

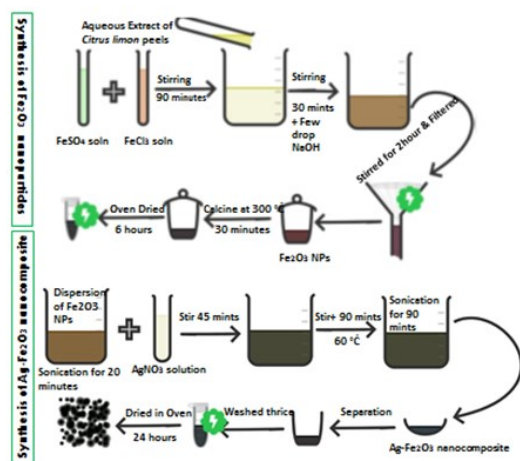
³Chemistry Department, University of Sahiwal-57000, Sahiwal Pakistan

Received: 14/11/2023, Accepted: 04/02/2024, Available online: 17/07/2024

*to whom all correspondence should be addressed: e-mail: tahsingulzar1@yahoo.com

<https://doi.org/10.30955/gnj.05516>

Graphical abstract



Abstract

In current study environment benign silver-iron oxide (Ag-Fe₂O₃) nanohybrid structures are fabricated as catalyst for CR dye decolorization. Industrial wastewater stream possesses several toxic dyes which are toxic carcinogen pollutants cause severe environmental disorders. Detoxification of Congo Red dye is carried out by silver-iron oxide nanohybrid structures having latent catalytic efficiency for dye decolorization. Silver iron oxide nanohybrid materials are fabricated from AgNO₃, FeSO₄/FeCl₃ and *Citrus limon* aqueous extract by doping AgNPs on Fe₂O₃ materials. For characterization of Ag-Fe₂O₃ nanostructures, UV-Visible, X-ray diffraction (XRD), Scanning electron microscope (SEM) and Fourier transform infrared (FT-IR) techniques are used. The crystallite size is measured from Debye Scherer equation and average size calculated is 54.3 nm. Furthermore, UV-Visible spectrophotometer is used to study the catalytic efficiency of Ag-Fe₂O₃ nanohybrid material which is observed to be >80% within 10 minutes. Moreover, parameters like contact time, dosage of catalyst, temperature and pH are measured to optimize reaction

conditions for the dye degradation by adding prepared nanohybrids. The kinetic studies were performed for the degradation reaction and were originate to follow first order kinetics. Reusability test is also applied to check the stability of nanohybrid catalyst that affirmed it to be as highly stable nanomaterial.

Keywords: Fabrication, Ag-Fe₂O₃, *Citrus limon*, Congo Red dye, Detoxification, Kinetics, Reusability test

1. Introduction

Nanomaterials (NMs) are known from decades for their ecosafe application regarding water and waste water treatments. Metal nanoparticles (MNPs) are widely used for the decontaminations of toxic organic pollutants like dyes from water system but the efficiency of hybrid NMs to degrade toxicants is found much greater than single metallic nanoparticles (Abu-Saada *et al.* 2022) MNPs. Approximately 0.7 million tons of dyes are discharged by textile industries into the water bodies annually across the world (Heidarpour *et al.* 2020). Dyes have found potential application in a wide range of fields, such as coloring the textile apparels, foods materials, paints, printing inks, paper and leathers etc. As a consequence of flow of industrial effluents into the water bodies without any preliminary treatment, water is getting contaminated with a number of toxic coloring materials. Industrial waste water contaminated with such toxic dyes is an alarming threat for the ecosystem. Due to rapid industrialization caused by growth in population, transportation and increasing demand for advanced life style, the release of these pollutants level has been enhanced in aquatic system (Nishida *et al.* 2017; Mahalingam and Ahn. 2018; Marimuthu *et al.* 2020; Muraro *et al.* 2020).

The pollution caused by dyes mostly contain highly stable polycyclic aromatic complex compounds (PACC), being non-biodegradable in nature hence leading to severe environmental issues (Dong *et al.* 2017; Cuerda-Correa *et al.* 2020). In order to ensure the preservation of aquatic

life and other related organisms, these organic dyes are needed to be treated (Kulkarni *et al.* 2017). Hence keeping in view hazardous impacts of these coloring compounds, number of dyes abatement strategies have been employed for dyes degradation (Zhang *et al.* 2014; Zhan *et al.* 2019; Kiran *et al.* 2020; Panda *et al.* 2023).

Among the available synthetic strategies, catalytic reduction following green chemistry principle and sustainable development is considered as a potential technique for the effective detoxification of these organic pollutants. Conventionally catalytic degradation involves the reduction of dyes in the presence of reducing agent such as NaBH_4 , but in green synthetic methods plant/plant parts aqueous extract act as reducing and stabilizing agent (Dong *et al.* 2017; Liu and Corma. 2018; Huston *et al.* 2021). Investigations made so far had disclosed various techniques for dye degradation, whereas MNPs have found potential applications in heterogeneous catalysis owed by their high surface area and fine tunable porosities (Khan *et al.* 2020; Shen *et al.* 2020; Xu *et al.* 2021). To further increase the catalytic efficiency, metal/metal oxide nanoparticles are modified into nanocomposites and nanohybrid materials. The fabrication of nano-sized metal nanoparticles into metal oxide nano-matrix, maximize the mechanical strength, surface area, conductivity and hence the catalytic efficiency of the nanocatalyst (Feng *et al.* 2017; Sallam *et al.* 2018, Rasool *et al.* 2023).

Iron oxide nanoparticles are recognized as efficient catalysts because of their excellent redox ability between Fe^{2+} and Fe^{3+} ions. Moreover, the magnetic properties of iron based oxides enhance its reusability (Subha *et al.* 2018). In literature, doping of noble metal on Fe_2O_3 nanostructure surface has been reported for generation of upto the mark properties. Silver nanoparticles (Ag NPs) have attained considerable attention due their non-toxic nature, and unique optical characteristics. Further Ag-NPs have diverse range of applications such as safe inorganic antibacterial agent, chemical, electronic, photo electrochemical, magnetic, antibacterial and biological labeling characteristics, catalytic, chemical sensor, food industries, agriculture, drug delivery, water treatment, textile industries etc. (Li and Yang. 2016; Liu *et al.* 2016; Nguyen *et al.* 2019). Preparation of Ag-NPs involves the reduction of silver ions into the corresponding zero valent atoms, whether in solution or gaseous environment in the presence of reducing agents. However, the reducing agents may secondarily lead to environmental and biological toxicity (Pillarisiti *et al.* 2019). Numerous studies have been focused on biosynthesis of Ag-NPs with potential applications in antimicrobial activities. In order to avoid the above mentioned issues, an environmentally benign green synthesis of Ag- Fe_2O_3 nanohybrids has been introduced. This strategy involves the use of plant extract as a reductant and capping agents for the formulation of MNPs (Kiran *et al.* 2018; Chand *et al.* 2020; Gaur *et al.* 2023).

This current research is focused on the synthesis of Ag- Fe_2O_3 nanohybrid structures by green method using *Citrus*

limon aqueous extract (Figure 1), their characterization followed by determination of catalytic efficiency of Ag- Fe_2O_3 nanohybrid catalyst for the detoxification of Congo Red dye (Figure 2) under optimum environmental reaction conditions (Panda *et al.* 2023).

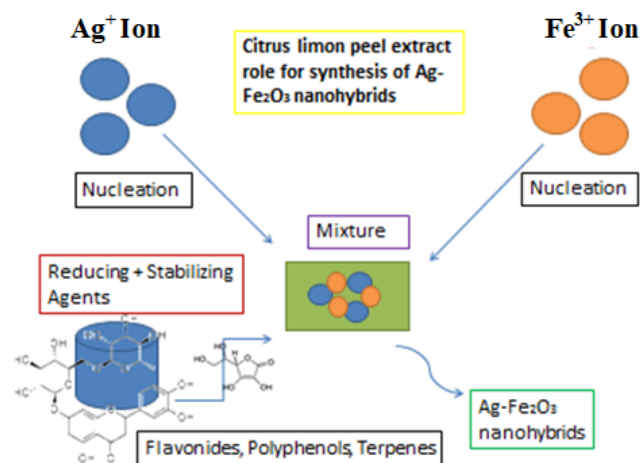


Figure 1. Role of *C. limon* fruit peels extract for the synthesis of Ag- Fe_2O_3 nanohybrids

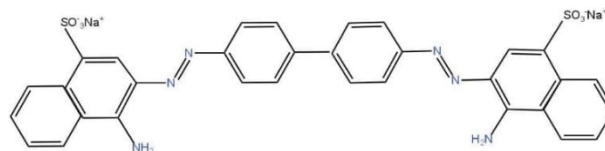


Figure 2. Structure of Congo Red dye

2. Materials and methods

2.1. Materials collection

Citrus limon (lemon) was purchased from local market of Faisalabad, Punjab, Pakistan. Ferrous sulphate heptahydrate ($\text{FeSO}_4 \cdot 7\text{H}_2\text{O}$), ferric chloride ($\text{FeCl}_3 \cdot 4\text{H}_2\text{O}$) and sodium hydroxide (NaOH) were obtained from Sigma Aldrich, Germany. Silver nitrate and sodium borohydride (NaBH_4) were purchased from Merck, USA. Congo red dye (Figure 2) was received from BDH chemicals, China. All the listed chemicals were pure, guaranteed and of analytical grades so used without any purification. Deionized water was used as a solvent throughout this work.

2.2. Synthesis of iron oxide nanoparticles

Fe_2O_3 nanomaterials were prepared according to the method described by Sallam *et al.* (2018) with some modifications according to requirement. In this method FeSO_4 and FeCl_3 salts solutions were used as precursor for the synthesis of Fe_2O_3 nanoparticles. For this purpose 0.8 g FeSO_4 and 1.45 g FeCl_3 were dissolved separately in 60 mL of the water at ambient atmospheric conditions. These two solutions were mixed and allowed to stir for 90 minutes. Then 20 mL aqueous extract of *C. limon* was added dropwise followed by swirling the mixture at moderate rate. Furthermore, few drops of 0.1 M NaOH were added slowly, followed by shaking for 30 minutes to maintain the pH upto 9.0. Appearance of black precipitates indicated the formation of Fe_2O_3 nanoparticles. The resultant iron oxide nanoparticles were further stirred for 120 minutes, collected, dried at 80°C for

120 minutes and then calcined at 300°C for 30 minutes using heat resistance muffle furnace. The product obtained was stored for further process (Ruiz-Baltazar *et al.* 2019; Kiran *et al.* 2020).

2.3. Fabrication of Ag-Fe₂O₃ nanohybrid

0.3 mg of previously prepared Fe₂O₃ nanoparticles were well-dispersed in 40 mL de-ionized water under ultrasonic treatment, then aqueous solution of AgNO₃ (0.04 g/15 mL) was added drop-wise into the dispersed nanoparticles suspension. The mixture formed was stirred for 45 minutes at 40°C, and then sonicated for 90 minutes. The resultant greenish black color Ag-Fe₂O₃ nanohybrids thus obtained, were washed thrice times with deionized water, and then dried in oven at 75°C for 24 hr as given in Figure 3 (Wang *et al.* 2020).

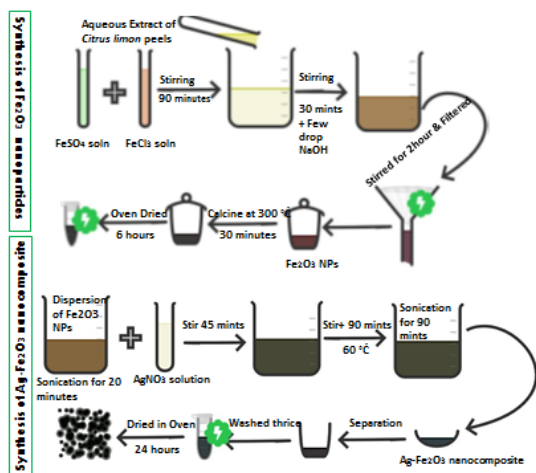


Figure 3. Scheme for the synthesis of Ag-Fe₂O₃ nanohybrids

2.4. Characterizations of Ag-Fe₂O₃ Nanohybrid materials

FTIR analysis is carried out using FTIR spectrum (Perkin Elmer, Germany) with resolution 0.5 cm⁻¹ using KBr pellet having frequency range of 400-4000 cm⁻¹ to analyze the functional groups present in the nanohybrid sample. The crystalline phase of nanohybrids and size are measured by X-ray diffractometer (XRD Bruker D8 advance Cu target Germany) functioning with CuK α radiation source ($\lambda = 1.54 \text{ \AA}$) produced at 40 KV and 40 mA. Scans are executed between 2 θ values ranged from 20°- 80° at the rate of 0.4 s per point. Morphology and average size of IONs, and nanohybrids are observed using scanning electron microscope (SEM Cube II EmCraft, South Korea) having resolution of 5.0 nm using SE detectors. CHNS analysis of the iron oxide nanoparticles and Ag-Fe₂O₃ nanohybrids are also performed for the detection of contaminants present in the sample using elemental analyzer 2400 (Perkin Elmer Germany), UV-Visible spectrophotometer (UV-Vis 2800, Cole Parmer USA).

2.5. Optimization of reaction parameters for decolorization of Congo Red dye

For the decolorization of Congo Red dye solution, the reaction conditions of Congo Red dye concentration (0.01% to 0.05% with 20 time dilution), Ag-Fe₂O₃ nanohybrids (0.001-0.01 g), pH (3- 8) and temperature (30- 80°C) were optimized. Only one experimental

parameter was varied by keeping other parameters constant.

2.6. Chemical Analysis

All experimental reactions were carried out in triplicate. The absorbance was measured at λ_{max} (497 nm). The % Decolorization was measured by the given formula

$$\text{Decolorization (\%)} = \frac{C_0 - C_t}{C_0} \times 100 \quad (1)$$

Where C_0 and C_t corresponds to the CR dye concentration at zero time and any time t , respectively, obtained from UV-Visible absorption peaks (Kiran *et al.* 2020; Rasool *et al.* 2023).

2.7. Mineralization Study

The treated and untreated Congo Red dye solution samples were subjected for water quality parameters like COD and TOC (Curic *et al.* 2021).

2.8. Dye degradation study

In catalytic degradation experiment of Congo Red dye, 5 mL of freshly prepared aqueous extract of *C. limon* (0.5 M) was added to 10 mL Congo Red dye solution (0.02 M). Now Ag-Fe₂O₃ nanohybrid (1 mM/10 mL) was added into the reaction mixture. The process of the reaction was continuously monitored with the help of UV-Visible spectrophotometer, until the complete de-colorization of the colored solution was achieved. Reduction reaction was performed in triplicate (Kiran *et al.* 2020; Ahmed *et al.* 2022). The Congo Red dye degradation was checked at different steps with bond breakage and newly formation of different bonds (Asses *et al.* 2018; Nadeem *et al.* 2022).

2.9. Statistical Analysis

All experimental parameters were checked in triplicate. Mean of triplicates were calculated and results computed using standard deviation and standard error (Al-Kordy *et al.* 2021).

3. Results and Discussion

3.1. Characterization of IONs and Ag-Fe₂O₃ nanohybrids

3.1.1. Scanning Electron Microscopy for Ag-Fe₂O₃ nanohybrids

The surface structure of the prepared pure Fe₂O₃ NPs and Ag-Fe₂O₃ nanohybrids have been determined using SEM. Figure 4a & b represents the image of Fe₂O₃ nanomaterials. It is evident that Fe₂O₃ is composed on the rough but compact spongy surfaces with irregular grain size. Ag-Fe₂O₃ nanohybrid possesses more spongy surfaces than Fe₂O₃ nanomaterials with reduced compactness. These porous surfaces enhance the active site and increase surface area of the silver coated iron oxide nanomaterials (IONs). Figure 4c & d expressed the SEM images of Ag-Fe₂O₃ nanohybrid material structures (Khan *et al.* 2020). It is depicted from the image that Ag is variably distributed at the IONs spongy surface hence exhibiting a good correlation that causes the formation of nanostructures. This interaction denotes compact structures, spongy structure and high energy materials. This random distribution of Ag over Fe₂O₃ nanoparticles is

considered to be responsible for the increase in the catalytic efficiency of the nanomaterial by increasing active sites. These sites are highly active for the adsorption of different dyes (Khan *et al.* 2020; Aragaw *et al.* 2021).

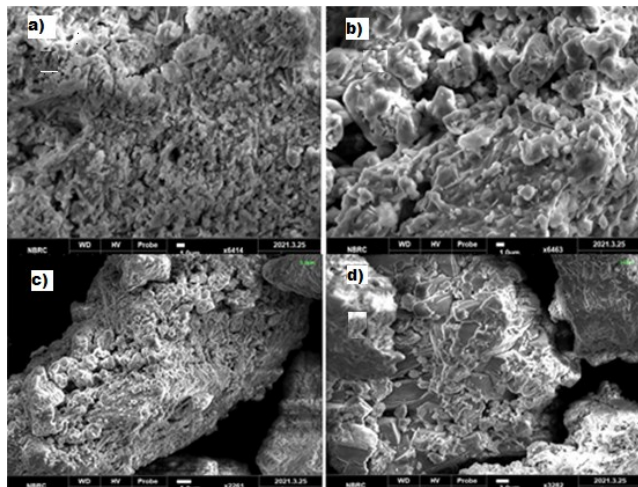


Figure 4. SEM micrograph for Fe_2O_3 (a,b) and $\text{Ag-Fe}_2\text{O}_3$ nanostructures (c,d)

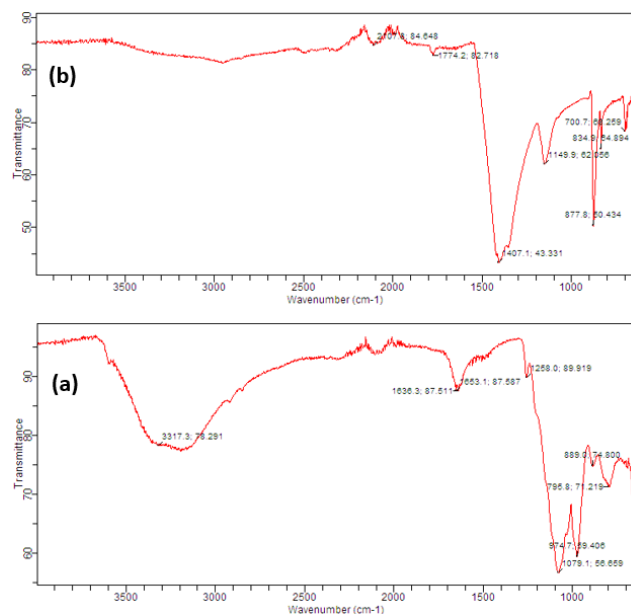


Figure 5. FTIR images of Fe_2O_3 (a) and $\text{Ag-Fe}_2\text{O}_3$ nanostructures (b)

3.1.2. FTIR Analysis

FTIR spectra of IONs and silver iron oxide nanoparticles nanostructures are shown in the Figure 5. Figure 5a represents the spectrum of IONs while Fig. 5b showed spectrum of nano hybrid structure also evident from literature reports (Uma *et al.* 2018). The iron oxide nanoparticles spectrum showed a broad band at 3317 cm^{-1} due to -OH functional group, a medium peak at 1636 cm^{-1} due to CO stretching vibration. A sharp peak at 1079 cm^{-1} and medium to sharp peak at 974 cm^{-1} were assigned to the C-O bond and due to C=C bond bending (Mahdavi *et al.* 2013). $\text{Ag-Fe}_2\text{O}_3$ nanomaterial showed a weak absorption band at 2107 cm^{-1} is due to aromatics overtone appeared in spectrum. A weak band absorption peak at 1774 cm^{-1} was due to C=O stretching. A strong FTIR absorption band appeared at 1407 cm^{-1} , attributed to

CH_2 asymmetric stretching. Another medium to strong peak appeared at 1149 cm^{-1} and 610 cm^{-1} for C-O stretching and for $\text{Ag-Fe}_2\text{O}_3$ nano hybrids (Javed *et al.* 2016; Khan *et al.* 2020; Nasiri K. 2023).

From spectra, it was observed that some new peaks appeared in the $\text{Ag-Fe}_2\text{O}_3$ nanostructures that were not present in IONs spectrum indicated the formation of nanostructures. Another -OH absorption peak disappeared in $\text{Ag-Fe}_2\text{O}_3$ nanostructures shown in Figure 5b indicated that product was completely moisture free. Another peak shifting is observed from 1653 cm^{-1} to 1774 cm^{-1} and 1079 cm^{-1} to 1149 cm^{-1} was due to C-O out of plane vibrational mode while absorption at 700 cm^{-1} indicated the formation of $\text{Ag-Fe}_2\text{O}_3$ nanostructures (Al-Zahrani *et al.* 2022).

3.1.3. X-Ray Diffraction (XRD) analysis

XRD analyses were performed for both IONs and $\text{Ag-Fe}_2\text{O}_3$ nanostructures as given in Figure 6 to check the crystallinity in the nano hybrid material. Figure 6 showed the spectrum of Fe_2O_3 NPs exhibiting characteristic diffraction peaks at 19.7° , 24.7° , 38.4° , 45.6° , 56.1° and 62.3° . Similarly Figure 5 also displayed $\text{Ag-Fe}_2\text{O}_3$ nanostructure XRD pattern with some new peaks at 12.9° , 23.2° , 33.4° , 52.1° , 60.9° and 69.3° that were absent in the iron oxide nanoparticles pattern convincing the formation of nanostructure hybrid material and were according to the XRD pattern found in the previous studies (Sallam *et al.* 2018; Feng *et al.* 2019). It should also be noted that some peaks have been attributed to both Ag and Fe_2O_3 produce similar peaks at same 2θ values, thus cannot be detected easily. The size of nano hybrid crystallite was calculated by Debye Scherer equation (1)

$$D = \lambda / \beta \cos \theta \quad (2)$$

where λ is the X-ray wavelength, β is the full width at half maximum (FWHM) height of a x-ray diffraction peak, θ is the diffraction angle while K is Scherer's equation constant which is equal to 0.9. The crystallite size obtained for the prepared $\text{Ag-Fe}_2\text{O}_3$ nano hybrids were found in the range $48.6\text{ nm} - 60.3\text{ nm}$ and average crystallite size was measured to be 54.3 nm which was in according to literature reports (Hosseinidoust *et al.* 2016; Abu-Saeda *et al.* 2022, Panda *et al.* 2022).

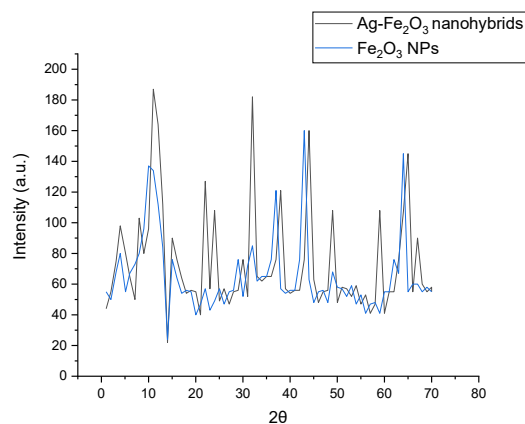


Figure 6. XRD pattern of a) IONs b) $\text{Ag-Fe}_2\text{O}_3$ nano hybrids

3.1.4. Measurements of λ_{max} for Congo Red dye

The absorbance of the Congo Red dye was monitored from 400- 780 nm, with the interims of 20 nm to find the wavelength exhibiting maximum absorbance. The λ_{max} was measured to be 497 nm (Figure 7).

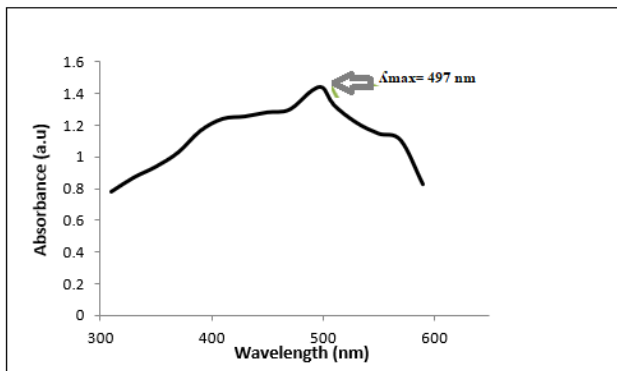


Figure 7. Measurement of λ_{max} of Congo Red dye

3.1.5. Catalyst efficacy for Congo Red dye decolorization

Ag-Fe₂O₃ nanohybrid materials are highly efficient against pollutants sensing and degradation so help in keeping ecosystem clean and safe. The production and inherit use of such nanohybrid materials using greener approach are the concern of today’s environmental scientists. Such method helps to open new doors to obtain multifunctionality and generate opportunity to study novel environmental physiochemical properties for next generation hybrid materials (Biswal *et al.* 2020; Hitkari *et al.* 2023).

The proposed dye degradation mechanism was presented in Figure 8. Figure 8 clearly depicts that dye might be degraded through several transition stated prior its conversion into final product.

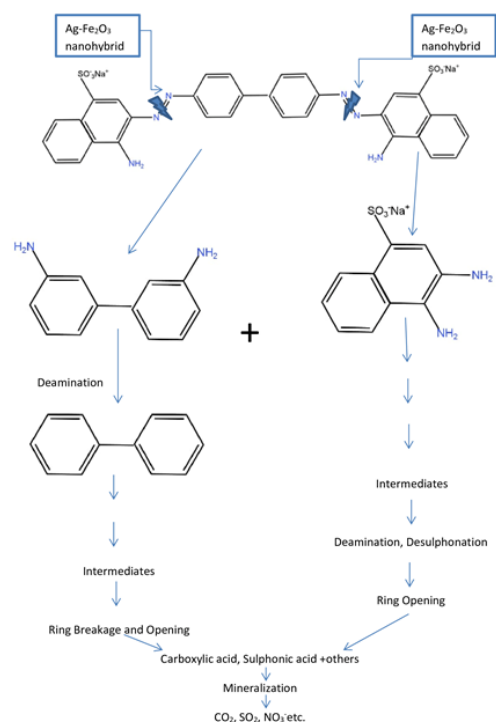


Figure 8. Proposed dye degradation mechanism

The catalyst efficiency of IONs and Ag-Fe₂O₃ nanohybrids were measured against Congo Red dye reduction using

spectrophotometer. For this purpose 10 mL of Congo Red dye solution was taken from stock solution to which 5 mL of freshly prepared *C. limon* aqueous extract solution was added. Further 0.01g of IONs was added to the above reaction mixture. Figure 9 expressed the UV-Visible spectrum of Congo Red dye at regular time interval of 2 minutes. By the addition of nanohybrids, the dye concentration was decreased that ultimately increase the % age degradation. The reduction property of IONs was observed in terms of decrease in absorption intensity at λ_{max} (497 nm) characteristics of Congo Red direct dye was shown in Figure 9. This decrease in the concentration of dye is attributed to the transformation and decolorization of the Congo Red dye due to its adsorption on the surface of catalyst. Initially a decrease in absorption peak was observed up to 10 min., after which no further change in peak height was noticed. In a second batch of reaction, 0.01g of Ag-Fe₂O₃ was added to Congo Red and *C. limon* aqueous extract to the reaction mixture. As in the earlier case, the reduction in peak intensity at 497 nm was regularly observed with the help of UV-Visible spectrophotometer exhibited in Figure 9a (Chand *et al.* 2020; Rasool *et al.* 2023).

Congo Red dye decolorization was comparatively robust when Ag-Fe₂O₃ nanohybrid catalyst was used, as given in Figure 9b. In the presence Ag-Fe₂O₃ nanohybrids, the complete disappearance of Congo Red absorption peak is achieved after 10 minutes. Thus, it can be concluded that catalytic efficiency of Ag-Fe₂O₃ for Congo Red dye reduction was greater than that of Fe₂O₃, which has been attributed to the high conductivity of earlier one, achieved as a result of doping of Ag onto the surface of IONs matrix (Kiran *et al.* 2020; Gaur *et al.* 2023).

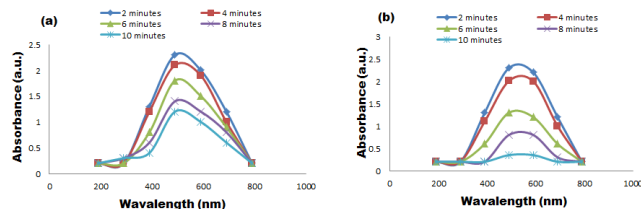


Figure 9. UV-Visible analysis Congo Red dye with time (a) presence of Fe₂O₃, (b) in presence of Ag-Fe₂O₃ nanohybrid structures

3.2. Optimization of reaction conditions for CR direct dye decolorization

Different physiochemical conditions were optimized for Congo Red dye decolorization (Figure 10) under study.

3.2.1. Effect of dye dose

Dye decolorization is an essential criterion for catalytic treatment of Congo Red dye. The effect of different dye concentration was measured (0.01%-0.05%) on decolorization of Congo Red dye. Dye decolorization was elevated from 65.6 % to > 80 % in 10 minutes as concentration was raised from 0.01% to 0.02% shown in Figure 10a. It is because of the adsorption of the dye on surface of catalyst increases as concentration increases upto optimum level. As catalyst concentration is increased further from 0.02%, decreased the dye decolorization was noticed. The raised dye concentration may cause

agglomeration hence reduced decolorization (Ghaffar *et al.* 2021; Kiran *et al.* 2021). At elevated concentration the dye molecules might cause inhibition due to poisoning of catalyst for the occupation of active sites. Hence may decrease the effectiveness of Ag-Fe₂O₃ nanohybrid structures (Ali *et al.* 2018; Al-Zahrani *et al.* 2023). Rasool *et al.* (2023) has also reported the similar investigation for the dye decolorization. Actually Congo Red dye molecules get adsorbed on the surface Ag-Fe₂O₃ nanohybrids. After that dye molecules acted as electrophilic reagent while nanohybrids act as relay system for the electron transfer and reducing agent act as nucleophilic reagent. This electron transfer because dye transformation and decolorization so converted into simpler byproducts (Gola *et al.* 2021; Huang Mu *et al.* 2023).

3.2.2. Effect of Ag-Fe₂O₃ nanohybrids catalyst dose

The amount of catalyst is a key factor for the dye decolorization. The enhanced catalyst has higher number of active sites which influence decolorization of dye in solution (Rafique *et al.* 2021). A number of tests were performed by changing the concentration of Ag-Fe₂O₃ nanohybrid catalyst from 1 mg/L to 10 mg/L. As catalyst quantity was enhancement from 0.001 to 0.005 g/L, Congo Red dye decolorization was amplified from about 12% to 89% and beyond this concentration no appreciable change in dye concentration was noted (Ghaffar *et al.* 2021). So Ag-Fe₂O₃ nanohybrid concentration (0.05%) was found to be optimal catalyst dose for Congo Red dye decolorization. The increase in catalyst dose enhances the number of active sites upto optimum concentration (Figure 10b). As catalytic site are functional upto certain limits which is evident from the catalyst efficacy for CR dye decolorization (Ahmed *et al.* 2022). It was also investigated that by increasing doped nanomaterials concentration the rate of dye degradation due to increasing the number of sites available on the catalyst behalf has also been reported (Chan *et al.* 2019; Hitkari *et al.* 2022). It was reported that the Congo Red dye degradation was accompanied by dissociation of chromophoric groups and transformation of the dye into low molecular mass products. As the results are in consistence with literature reviewed for dye degradation. The mechanism of Congo Red dye decolorization might be due to the creation of surface plasmonic resonance excitation within the molecular environment (Jiang *et al.* 2021; Dharshini *et al.* 2023).

3.2.3. Effect of pH

pH has significant action on the decolorization of Congo Red dye in solution. The reaction under investigation is largely dependent on the pH of dye solution. The changes in the pH of solution cause the charging of Ag-Fe₂O₃ nanohybrids and shift the probabilities of the reaction under investigation (Kiran *et al.* 2018). The Congo Red dye reduction was observed to be increased upto 86.3% by varying pH from 1-5. When pH increased from 6 to 8 the direct Congo Red dye reduction was decreased. So pH 6 is considered as optimum pH for the reduction of Congo Red dye given in Figure 10c. It is revealed from literature studies that the dye decolorization is unfit in basic

medium and in higher acidic medium and lower acidic medium favors the Congo Red dye decolorization. Hence catalytic efficacy of mix metal and metal oxide largely affected by the pH of the dye solution under observation (Azeez *et al.* 2018). In comparison with literature Ali *et al.* (2022) found that the production of ·OH free radical at pH >7 enhances the degradation of Congo Red molecules. Hence, the obvious inclined in the process at higher pH > 9 is credited to the negatively charged surface of the nanohybrid catalyst due to OH aggregation in solution. Therefore, an electrostatic repugnance force was developed between the negatively charged Congo Red molecules and the negatively charged surfaces catalyst (Kiran *et al.* 2020; Rasool *et al.* 2023).

3.2.4. Effect of Temperature

Temperature is a crucial parameter that can affect the decolorization of dyes. The present work was studied under the optimized conditions of dye concentration, catalyst dose and pH. The decolorization of Congo Red was studied under temperature ranges from 30°C to 80°C. Optimum Congo Red direct dye decolorization (89.5%) was achieved at 40°C and at higher temperatures decolorization of Congo Red dye was reduced. The direct dye decolorization was first increased and then decreased (Figure 10d). The decreased concentration of Congo Red dye at higher than 40°C can be considered due to loss of catalytic active sites on Ag-Fe₂O₃ nanohybrid structures (Rafique *et al.* 2021). Debnath and Mondal (2020) have also studied the outcome of temperature on the removal of Congo Red dye by nanoparticles and reported similar results. It was also investigated that by increasing temperature the dye decolorization also increased due to increase in the mesoporous nature that destroyed at elevated temperature (Chan *et al.* 2019; Dharshini *et al.* 2023).

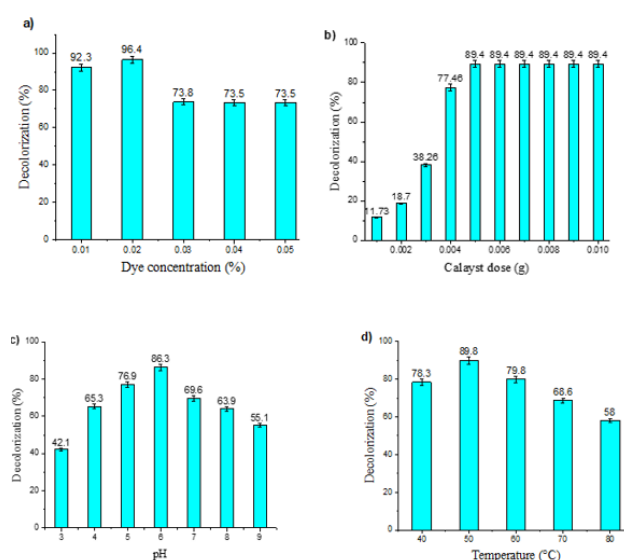


Figure 10. Optimization of reaction parameters a) Dye dose concentration b) Dose of catalyst c) reaction pH d) optimization of Temperature

3.2.5. Mineralization Study

Mineralization efficacy is estimated using quality parameters like TOC and COD. Percent reduction in COD

and TOC is measured through contact time from two to fifteen minutes as illustrated in Figure 11. As contact time is increased, % reduction of the Congo Red dye also enhanced. % Removal of Congo Red dye is amplified from 8 to 10 minutes and then decrease is observed upto 15 minutes as shown in Figure 11. It may be due to the inhibition factor caused by side products formed that slower the process. Larger values of COD and TOC illustrated that Ag-Fe₂O₃ nanohybrid has reduced the dye through various intermediates during reaction (Debnath and Mondal. 2020; Nadeem *et al.* 2022). The % reduction of the target Congo Red dye in COD and TOC was monitored by changing time from 10-70 mints. It was noticed that the dye reduction was increased from 10-50 mints evident from the Figure 11. Further increase in time decreased % reduction of COD and TOC. The percentage dye reduction in COD and TOC was achieved by 80% and 90% that degraded by nanohybrids materials synthesized from *C.limon* (Dharshini *et al.* 2023; Rasool *et al.* 2023). It is due to the conversion of dye molecules from complex to simpler and less toxic products thus leading to the mineralization of dye upto maximum extent (Sumi *et al.* 2016; Kishore *et al.* 2021; Shokoohi *et al.* 2021).

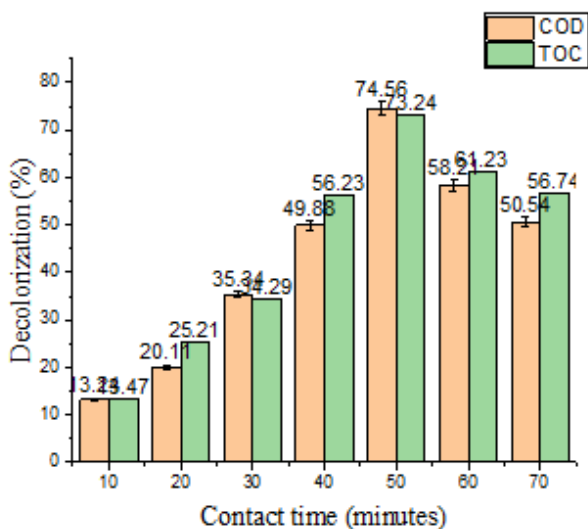


Figure 11. Quality parameter study for COD and TOC

3.2.6. Kinetics Interpretation for Congo Red dye decolorization

Kinetic studies for the Congo Red dye degradation by Ag-Fe₂O₃ nanohybrid structures as catalyst have been performed on the data obtained through experiment. The experimental data of Congo Red degradation is received by spectrophotometric measurements and is treated to find order of the Congo Red degradation reaction using different equations. Figure 12 shows Congo Red dye concentration at various time interval using Ag-Fe₂O₃ nanostructures as catalyst. As the line denotes to linearly fits to the absorption experimental data. It is observed from the Figure 12a that the data does not properly follow the fitted line, exhibiting that reaction does not follow kinetics for zero order. Figure 12b plotted ln[dye] against time for Congo Red dye reduction in the solution using nanostructure as active catalyst. Similarly, Figure 14 c shows the data between 1/[dye] versus time for Congo

red dye degradation using nanocatalyst. The slope values for zero, 1st and 2nd order reactions are 0.372, 0.399 and 0.162, respectively. The greatest value of regression constant R² is 0.399 in Figure 12b, representing that the CR decolorization reaction has followed first order reaction kinetics. Therefore, the highest reduction reaction rate k for Congo Red decolorization reaction using Ag-Fe₂O₃ nanohybrid structure as catalyst is 0.3993 min⁻¹ (Khan *et al.* 2020; Kamal *et al.* 2021)

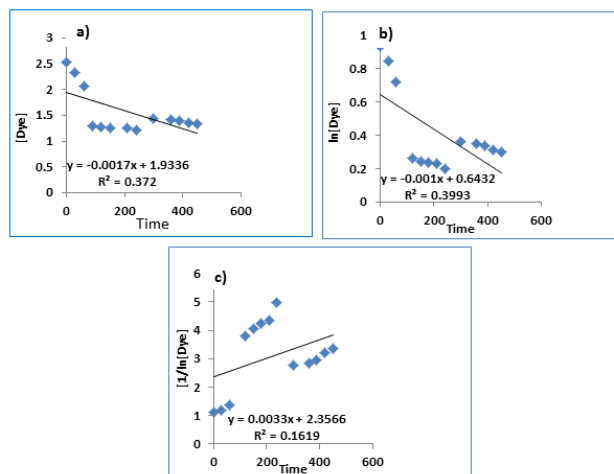


Figure 12. Absorbance linear data fitting of CR reduction by Ag-Fe₂O₃ nanostructure catalyst to the (a) zero order (b) first order and (c) second order kinetics

3.2.7. Reusability test for Ag-Fe₂O₃ nanohybrid catalyst

Catalyst reusability is a vital parameter to check catalytic efficiency and stability of a catalyst. As Ag-Fe₂O₃ nanohybrid has expressed good catalytic functionality but along with it, it is essential to check stability and efficiency of Ag-Fe₂O₃ nanohybrid structures as well. Hence catalyst is separated, washed and reused for Congo Red dye decomposition upto five cycles as displayed in Figure 13. It is cleared that Ag-Fe₂O₃ nanohybrid exhibited more than 80 % detoxification in all experimental series that showing chemical inertness and stability of catalyst in aqueous solution also reported previously (Anjum *et al.* 2021; Khalil *et al.* 2021; Ahmed *et al.* 2022).

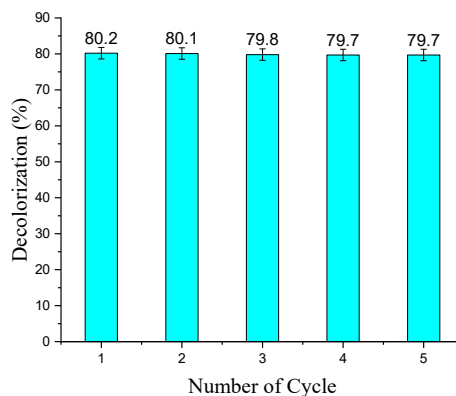


Figure 13. Catalyst Stability test

3.2.8. Toxicity Analysis

The biological membrane is majorly stabilized by hydrophobic force that holds lipid bilayer and

hydrophobic tail of phospholipids jointly. Further polar heads of phospholipids, water molecule and weekly attractive forces are responsible to sustain the subunits of the membrane *in vivo* and *in vitro*. The best way to determine lysis of a cell is by *in vitro* study. It is well-known facts that cell lysis occurs as a result of local vermin and microbial substances that attacks on the red blood cells effectively in contagious conditions. The erythrocytic covering is a dynamic configuration in and its own which can grasp critical variations at the interface, well established by green nanomaterial. The hemolysis rate is the observation of toxicity of different amounts of synthesized compounds on human red blood cells. The sample under investigation is taken on the x-axis along with positive control having lysis 100% and lysis of red blood cells on the y-axis. The hemolysis rate of the required dye sample by Ag-Fe₂O₃ nanohybrid was measured in present study to find toxicity of the nanohybrid material. Triton X-100 was used as positive control and PBS was taken as negative control depicting degradation 91.15% and 0% respectively. From Figure 14. It is cleared that there was an observable decrease in the toxicity of material as compared to positive and negative control samples that were successfully decomposed by silver iron oxide nanohybrids being as environmental benign and cleaning method (Jiang *et al.* 2021; Rasool *et al.* 2023).

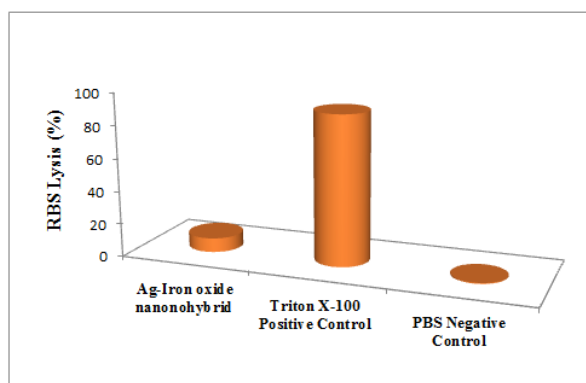


Figure 14. Toxicity test for the synthesized Ag-Fe₂O₃ nanohybrid catalyst

4. Conclusion

The development of eco-friendly, biodegradable, cost-efficient nanohybrids are gaining attention to remove hazardous environmental pollutants. Ag-Fe₂O₃ nanohybrids have been successfully fabricated by green method for environmental remediation. IONs and Ag-Fe₂O₃ nanohybrid catalyst were formulated by simple and green chemical method using aqueous extract of *Citrus limon*. The SEM images of Ag-Fe₂O₃ revealed the preparation of irregular spongy surface nanohybrids having 54.3 nm average particle size. The SEM image of Ag coated IONs depicted the smooth Ag distribution over the porous surface of IONs that enhance the active sites. Further it is evident that Ag distributed and studded in the porous spongy IONs surfaces hence enhancing catalytic efficiency of synthesized nanomaterial. The shift in the position of the peaks in FTIR spectrum at 610.3 cm⁻¹ from 710.1 cm⁻¹ indicates the formulation of Ag-Fe₂O₃

nanostructures. The appearance of new peaks at 23.2°, 33.4°, 52.1°, 60.9° and 69.3° in XRD depicted the formation of hybrid nanomaterials. So it is clear from all analytical techniques that green Ag-Fe₂O₃ nanohybrids were successfully fabricated. Ag-Fe₂O₃ nanohybrid materials were successfully used for the removal of Congo Red dye from aqueous solution under optimal reaction conditions. Hence Ag-Fe₂O₃ nanohybrid materials are playing the crucial role in the waste water purifications for environment remediation. The tailored designing of nanohybrids are constructed with physicochemical alteration and enables the nano-bioadsorbent with high dye removal specificity and efficiency. In present work the results indicate that Ag-Fe₂O₃ nanohybrid materials are more efficient (> 85 %) than simple Fe₂O₃ nanoparticles for degradation of textile Congo Red carcinogenic dye (> 65 %) hence helps in environmental remediation's. The current work proved to be an environmental benign approach for the reduction of toxicants in main water stream. This work suggests the environmental remediation from dyes for clean environment. It can be measured that nanohybrids can be employed for dyes remediation. Phytogenic synthesis of nanohybrid is eco-friendly approaches as higher surface area increase its potential work for wastewater treatment. The green synthesis of metal oxide nanomaterials and their application for dye degradation attracting great interest due to minimal waste and sustainable approach.

Authors Contributions

Mr. Faraz Ahmed has conducted experiments and improved the manuscript according to the technical guidance. Dr. Tahsin Gulzar and Dr. Tahseen Kamal, Dr. Shumaila Kiran and Dr. Ikram Ahmad have contributed equally and supervised keenly regarding the technical work. They helped in the technical evaluation of data and improving the manuscript write up and carrying out experiments and analyzed the experimental data of the research work enthusiastically.

Availability of data and materials

As this is the part of Ph.D studies of Mr. Faraz Ahmed so the whole data is present in his Ph.D thesis.

Declaration

Ethical Approval

All authors comprising the supervisory committee confirm that this manuscript is a part of Ph.D studies of Mr. Faraz Ahmed.

Consent to Participate and Publish

All authors have jointly contributed during Ph.D studies of Mr. Faraz Ahmed and affirm consents to publish this work in your esteemed journal.

Competing Interests

There is no conflict of interest among any of the authors.

Financial Support

No funds or grants are received for conducting this research work.

Acknowledgment

This research work was carried out at Department of Applied Chemistry, Government College University Faisalabad, Pakistan. I am thankful to Applied Chemistry Department for providing research facilities. All contributing authors are grateful to Dr. Tahsin Gulzar for lab equipment's to carry out smooth work.

References

- AbuSaeda N., Ahmad M.A. and Elmahgary M.G. (2022). Synthesis and characterization of novel magnetic nanoparticles for photocatalytic degradation of indigo carmine dye. *Material Science for Energy Technologies*, **5**, 116-124. <https://doi.org/10.1016/j.mset.2022.01.001>
- Ahmed F., Gulzar T., Kiran S., Ahmad I., Fatima A., Yasir S., Alhajaim W.F., Khalil A., Islam M., Bakhsh E.M. and Kamal T. (2022). Nickel oxide and carboxymethyl cellulose composite beads as catalyst for pollutant degradation. *Applied Nanoscience*, 1-11. DOI: 10.1007/s13204-022-02345-5
- Ali F., Khan S.B., Kamal T., Alamry K.A., Bakhsh E.M., Asiri A.M. and Sobahi T.R. (2018). Synthesis and characterization of metal nanoparticles templated chitosan-SiO₂ catalyst for the reduction of nitrophenols and dyes. *Carbohydrate Polymers*, **192**, 217-230.
- Ali M.H.H., Goher M.E., Al-Affy A.D.G. and El-Sayed S.M. (2022). A facile method for synthesis rGO/Ag nanocomposite and its uses for enhancing photocatalytic degradation of Congo red dye. *SN Applied Sciences*, **4**, 276. <https://doi.org/10.1007/s42452-022-05163-0>
- Al-Kordy H.M.H., Sabry S.A. and Mabrouk M.E.M. (2021). Statistical optimization of experimental parameters for extracellular synthesis of zinc oxide nanoparticles by a novel haloaliphilic *Alkalibacillus* sp.W7. *Science Reports*, **11**, 10924. <https://doi.org/10.1038/s41598-021-90408-y>
- Alzahrani E.A., Nabi A., Kamli M.R., Albukhari S.M., Althabaiti S.A., Al-Harbi S.A., Khan I. and Malik M.A. (2023). Facile green synthesis of ZnO NPs and plasmonic Ag-supported ZnO nanocomposite for photocatalytic degradation of methylene blue. *Water*, **15**(3), 384.
- Al-Zahrani F.A.M., Salem S.S., Al-Ghamdi H.A., Nhari L.M. and El-Shishtawy R.M. (2022). Green Synthesis and Antibacterial Activity of Ag/Fe₂O₃ Nanocomposite Using *Buddleja lindleyana* Extract. *Bioengineering*, **9**, 452.
- Anjum F., Asiri A.M., Khan M.A., Khan M.I., Khan S.B., Akhtar K., Bakhsh E.M., Alamry K.A., Alfifi S.Y. and Chakraborty S. (2021). Photo-degradation, thermodynamic and kinetic study of carcinogenic dye via zinc oxide/graphene oxide nanocomposites. *Journal of Material Research and Technology*, **15**, 1371-1391.
- Aragaw T.A., Bogale F.M. and Aragaw B.A. (2021). Iron-based nanoparticles in wastewater treatment: A review on synthesis methods, applications, and removal mechanisms. *Journal of Saudi Chemical Society*, **25** (8), 101280. DOI:10.1016/j.jscs.2021.101280
- Asses N., Ayed L., Hkiri N. and Hamdi M. (2018). Congo Red decolorization and detoxification by *Aspergillus niger*. Removal mechanism and dye degradation pathway. *BioMedical Research International*, 3049686. <https://doi.org/10.1155/2018/3049686>
- Azeez F., Al-Hetlani E., Arafah M., Abdelmonem Y., Nazeer A.A., Amin M.O. and Madkour M. (2018). The effect of surface charge on photocatalytic degradation of methylene blue by using chargeable titania nanoparticles. *Science Report*, **8**, 7104.
- Biswal S.K., Panigrahi G.K. and Sahoo S.K. (2020). Green synthesis of Fe₂O₃-Ag nanocomposite using *Psidium guajava* leaf extract: An eco-friendly and recyclable adsorbent for remediation of Cr(VI) from aqueous media. *Biophysical Chemistry*, **263**, 106392 DOI:10.1016/j.bpc.2020.106392
- Chan Y.Y., Pang Y.L., Lim S., Lai C.W., Abdullah A.Z. and Chong W.C. (2019). Biosynthesized Fe- and Ag-doped ZnO nanoparticles using aqueous extract of *Clitoria ternatea* Linn for enhancement of sonocatalytic degradation of Congo red. *Environmental Science and Pollution Research*. Doi:10.1007/s11356-019-06583-z
- Chand K., Cao D., Fouad E.D., Shah H.A., Dayo Q.A., Zhu K., Lakhan N.M., Mehdi G. and Dong S. (2020). Green synthesis, characterization and photocatalytic application of silver nanoparticles synthesized by various plant extracts. *Arabian Journal of Chemistry*, **13**(11), 8248-8261. DOI:10.1016/j.arabj.2020.01.009
- Cuerda-Correa E.M., Alexandre-Franco M.F. and Fernández-González C. (2020). Advanced Oxidation Processes for the Removal of Antibiotics from Water. An Overview. *Water*, **12**(1), 102. DOI:10.3390/w12010102
- Curic I., Dollar D. and Karadakik K. (2021). Textile wastewater reusability in knitted fabric washing process using UF membrane technology. *Journal of Cleaner Production*, **299**, 126899.
- Debnath P. and Mondal N.K. (2020). Effective removal of congo red dye from aqueous solution using biosynthesized zinc oxide nanoparticles. *Environment Nanotechnology and Monitoring Management*, 100320. Doi:10.1016/j.enmm.2020.100320
- Dharshini R.S., Poonkothai M., Srinivasan P., Mythili R., Syed A., Elgorban A.M., Selvankumar T. and Kim W. (2023). Nano-decolorization of methylene blue by *Phyllanthus reticulatus* iron nanoparticles: an eco-friendly synthesis and its antimicrobial, phytotoxicity study. *Applied Nanoscience*, **13** (3), 2527-2537.
- Dong Y.Y., Liu S., Liu Y.J., Meng L.Y. and Ma M.G. (2017). Ag@Fe₃O₄@cellulose nanocrystals nanocomposites: Microwave-assisted hydrothermal synthesis, antimicrobial properties, and good adsorption of dye solution. *Journal of Material Science*, **52** (13), 8219-8230. DOI:10.1007/s10853-017-1038-1
- Feng J., Fan D., Wang Q., Ma L., Wei W., Xie J. and Zhu J. (2017). Facile synthesis silver nanoparticles on different xerogel supports as highly efficient catalysts for the reduction of p-nitrophenol. *Colloids Surf. A Physicochemical Engineering Aspect*, **520**, 743-756. DOI:10.1016/j.colsurfa.2017.02.041
- Gaur J., Vikrant K., Kim K.H., Kumar S., Pal M., Badru R., Masand S. and Momoh J. (2023). Photocatalytic degradation of Congo red dye using zinc oxide nanoparticles prepared using *Carica papaya* leaf extract. *Materials Today Sustainability*, **22**, 100339. <https://doi.org/10.1016/j.mtsust.2023.100339>
- Ghaffar A., Kiran S., Rafique M.A., Iqbal S., Nosheen S., Hou Y., Afzal G., Bashir M., and Aimun U. (2021). Citrus paradise fruit peel extract mediated green synthesis of copper nanoparticles for remediation of Disperse Yellow 125 dye. *Desalination Water Treatment*, **212**, 368-375.

- Gola D., kriti A., Bhatt N., Bajpai M., Singh A., Arya A., Chauhan N., Srivastava S.K., Tyagi P.K. and Agrawal Y. (2021). Silver nanoparticles for enhanced dye degradation. *Current Research in Green and Sustainable Chemistry*, **4**, 100132. <https://doi.org/10.1016/j.crgsc.2021.100132>.
- Heidarpour H., Golizadeh M., Padervand M., Karimi A., Vossoughi M. and Tavakoli M.H. (2020). In-situ formation and entrapment of Ag/AgCl photocatalyst inside cross-linked carboxymethyl cellulose beads: A novel photoactive hydrogel for visible-light-induced photocatalysis. *Journal of Photochemistry and Photobiology A: Chemistry*, **398**, 112559. DOI:10.1016/j.jphotochem.2020.112559
- Hitkari G., Chowdhary P., Kumar V., Singh S. and Motghare A. (2022). Potential of Copper-Zinc Oxide nanocomposite for photocatalytic degradation of Congo Red dye. *Cleaner Chemical Engineering*, **1**, 100003. <https://doi.org/10.1016/j.clce.2022.100003>.
- Hosseinioust Z., Basnet M., Ven T.G., Van M. and Tufenkji N. (2016). One-pot green synthesis of anisotropic silver nanoparticles. *Environmental Science and Nanotechnology*, **3** (6), 1259-1264. DOI:10.1039/C6EN00112B
- Huang-Mu L., Devanesan S., Farhat K., Kim W. and Sivarasan G. (2023). Improving the efficiency of metal ions doped Fe₂O₃ nanoparticles: Photocatalyst for removal of organic dye from aqueous media. *Chemosphere*, **337**, 139229. <https://doi.org/10.1016/j.chemosphere.2023.139229>.
- Huston M., DeBella M., DiBella M. and Gupta A. (2021). Green Synthesis of Nanomaterials. *Nanomaterials*, **11**(8), 2130 DOI:10.3390/nano11082130
- Javaid R., Yaqub U. and Kawasaki S. (2016). Highly efficient decomposition of Remazol brilliant blue R using tubular reactor coated with thin layer of PdO. *Journal of Environmental Management*, **180**, 551-556.
- Jiang T., Lin Y., Amadei C.A., Gou N., Rahman S.M., Lan J., Vecitis C.D. and Gu A.Z. (2021). Comparative and mechanistic toxicity assessment of structure-dependent toxicity of carbon-based nanomaterials. *Journal of Hazardous Materials*, **418**, 126282. <https://doi.org/10.1016/j.jhazmat.2021.126282>.
- Kamal T., Asiri A.M. and Ali N. (2021). Catalytic reduction of 4-nitrophenol and methylene blue pollutants in water by copper and nickel decorated polymer sponges. *Spectrochimica Acta Part A: Molecular and Biomolecular Spectroscopy* **261**, 120019.
- Khalil A., Ali N., Asiri A.M., Kamal T., Khan S.B. and Ali J. (2021). Synthesis and catalytic evaluation of silver@nickel oxide and alginate biopolymer nanocomposite hydrogel beads. *Cellulose*, **28**, 11299-11313.
- Khan A.U., Rahman A., Yuan Q., Ahmad A., Khan Z.U.H., Mater H.M., Mahnashi M.H., Alyami B.A., Alqahtani Y.S., Ullah, S. and Wirman A.P. (2020). Facile and eco-benign fabrication of Ag/Fe₂O₃ nanocomposite using *Algaia Monozyga* leaves extract and its' efficient biocidal and photocatalytic applications. *Photodiagnosis and Photodynamic Therapy*, **32**, 101970.
- Khan F., Khan M.S., Kamal S., Arshad M., Ahmad S.I. and Nami S.A.A. (2020). Recent advances in graphene oxide and reduced graphene oxide based nanocomposites for the photodegradation of dyes. *Journal of Materials Chemistry C*, **8**(45), 15940-15955. DOI:10.1039/D0TC0368
- Kiran S, Nosheen S, Iqbal S, Abrar S, Jalal F, Gulzar T, Naseer N (2018). Photocatalysis using titanium dioxide for treatment of textile wastewater containing disperse dyes. *Chiang Mai Journal of Science*, **45**, 2730-2739.
- Kiran S., Rafique M.A., Iqbal S., Nosheen S. and Naz A. (2020). Synthesis of nickel nanoparticles using *Citrullus colocynthis* stem extract for remediation of reactive yellow 160 dye. *Environmental Science and Pollution Research*, 1-10.
- Kishore R., Purchase D., Dattatraya G., Saratale G.D., Saratale R.G., Ferreira L.F.R., Bilal M., Chandra R. and Bharagava R.N. (2021). Ecotoxicological and health concerns of persistent coloring pollutants of textile industry wastewater and treatment approaches for environmental safety. *Journal of Environmental Chemical Engineering*, **9** (2), 105012. <https://doi.org/10.1016/j.jece.2020.105012>.
- Kulkarni S., Jadhav M., Raikar P., Barretto D.A., Vootla S.K. and Raikar U.S. (2017). Green synthesized multifunctional Ag@Fe₂O₃ nanocomposites for effective antibacterial, antifungal and anticancer properties. *New Journal of Chemistry*, **41**(17), 9513-9520. DOI:10.1039/C7NJ01849E
- Li W.H. and Yang N. (2016). Green and facile synthesis of Ag-Fe₃O₄ nanocomposites using the aqueous extract of *Crataegus pinnatifida* leaves and their antibacterial performance. *Materials Letter*, **162**, 157-160. DOI:10.1016/j.matlet.2015.09.064
- Liu L. and Corma A. (2018). Metal Catalysts for Heterogeneous Catalysis: From Single Atoms to Nanoclusters and Nanoparticles. *Chemical Reviews*, **118** (10), 4981-5079. DOI:10.1021/acs.chemrev.7b00776
- Liu S., Chen Y. and Dong L. (2016). Ag-Fe₂O₃ nanocomposites with enhanced catalytic activity for reduction of 4-nitrophenol. *Material Research Express*, **3** (7), 075024. DOI:10.1088/2053-1591/3/7/075024
- Li V., Divya K., Gayathri S., Mohan J.E., Keerthana N., Vinitha M., Kirubanandan S. and Renganathan S. (2018). Applications of iron oxide nano composite in waste water treatment—dye decolourisation and anti-microbial activity. *MOJ Drug Design Develop and Therapy*, **2** (5), 178-184.
- Mahdavi M., Namvar F., Ahmad M.B. and Mohamad R. (2013). Green Biosynthesis and Characterization of Magnetic Iron Oxide (Fe₃O₄) Nanoparticles Using Seaweed (*Sargassum muticum*) Aqueous Extract. *Molecules*, **18**, 5954-5964. DOI:10.3390/molecules18055954
- Mahalingam S. and Ahn Y.H. (2018). Improved visible light photocatalytic activity of rGO-Fe₃O₄-NiO hybrid nanocomposites synthesized by in situ facile method for industrial wastewater treatment applications. *New Journal of Chemistry*, **42** (6), 4372- 4383. DOI:10.1039/C8NJ00013A
- Marimuthu S., Antonisamy A.J., Malayandi S., Rajendran K., Tsai P.C., Pugazhendhi A. and Ponnusamy V.K. (2020). Silver nanoparticles in dye effluent treatment: A review on synthesis, treatment methods, mechanisms, photocatalytic degradation, toxic effects and mitigation of toxicity. *Journal of Photochemistry and Photobiology B: Biology*, **205**, 111823. DOI:10.1016/j.jphotobiol.2020.111823
- Muraro P.C.L., Mortari S.R., Vizzotto B.S., Chuy G., Santos D.C., Brum L.F.W. and Silva W.L. (2020). Iron oxide nanocatalyst with titanium and silver nanoparticles: Synthesis, characterization and photocatalytic activity on the degradation of Rhodamine B dye. *Science Report*, **10**. DOI: 10.1038/s41598-020-59987-0

- Nadeem F., Fozia F., Aslam M., Ahmad I., Ahmad S., Ullah R., Almutairi M.H., Aleya L. and Abdel-Daim M.M. (2022). Characterization, Antiplasmodial and Cytotoxic Activities of Green Synthesized Iron Oxide Nanoparticles Using *Nephrolepis exaltata* Aqueous Extract. *Molecules*, **27**, 4931. <https://doi.org/10.3390/molecules27154931>
- Nasiri K. (2023). Synthesis of Ag-Fe₂O₃ nanoparticles with antibacterial and antifungal impacts on dental microbia. *Nanomedicine Research Journal*, **8** (3), 283-289.
- Nguyen T.N.L., Do T.V., Nguyen T.V., Dao P.H., Trinh V.T., Mac V.P., Nguyen A.H., Dinh D.A., Nguyen T.A., Vo T.K.A., Tran D.L. and Le T.L. (2019). Antimicrobial activity of acrylic polyurethane/Fe₃O₄-Ag nanocomposite coating. *Progress Organic Coatings*, **132**, 15-20. DOI:10.1016/j.porgcoat.2019.02.023
- Nishida N., Amagasa S., Kobayashi Y. and Yamada Y. (2017). Mixture of silver and iron oxide nanoparticles produced by chemical methods. *Hyperfine Interactions*, **238** (1), 1-7. DOI:10.1007/s10751-017-1445-3
- Panda B., Mondal D., Mandal, S. et al. (2022). One-pot solution combustion synthesis of porous spherical-shaped magnesium zinc binary oxide for efficient fluoride removal and photocatalytic degradation of methylene blue and Congo red dye. *Environmental Science and Pollution Research*, **30**, 81386-81402. <https://doi.org/10.1007/s11356-022-22551-6>.
- Pillarisetti S., Uthaman S., Huh K.M., Koh Y.S., Lee S. and Park I. (2019). Multimodal Composite Iron Oxide Nanoparticles for Biomedical Applications. *Tissue Engineering and Regenerative Medicine*, **16** (5), 451- 465. DOI:10.1007/s13770-019-00218-7.
- Rafiq A., Ikram M., Ali S., Niaz F., Khan M., Khan Q. and Maqbool M. (2021). Photocatalytic degradation of dyes using semiconductor photocatalysts to clean industrial water pollution. *Journal of Industrial and Engineering Chemistry*, **97**, 111-128. <https://doi.org/10.1016/j.jiec.2021.02.017>
- Rafique M.A., Jamal A., Ali Z., Kiran S., Iqbal S., Nosheen S., Ansar Z. and Hossain B. (2022). Biologically Synthesized Copper Nanoparticles Show Considerable Degradation of Reactive Red 81 Dye: An Eco-Friendly Sustainable Approach. *BioMedical Research International*, 1-9. DOI: 10.1155/2022/7537955
- Rasool A., Kiran S., Gulzar T., Abrar S., Ghaffar A., Shahid M., Nosheen S. and Naz S. (2023). Biogenic synthesis and characterization of ZnO nanoparticles for degradation of synthetic dyes: A sustainable environmental cleaner approach. *Journal of Cleaner Production*, **398**, 136616. <https://doi.org/10.1016/j.jclepro.2023.136616>.
- Ruíz-Baltazar Á.d.J., Reyes-López S.Y., Mondragón-Sánchez M.L., Robles-Cortés A.I. and Pérez R. (2019). Eco-friendly synthesis of Fe₃O₄ nanoparticles: Evaluation of their catalytic activity in methylene blue degradation by kinetic adsorption models. *Results in Physics*, **12**, 989-995. DOI:10.1016/j.rinp.2018.12.037
- Sallam S. A., El-Subruiti G. M. and Eltaweil A. S. (2018). Facile Synthesis of Ag-γ-Fe₂O₃ Superior Nanocomposite for Catalytic Reduction of Nitroaromatic Compounds and Catalytic Degradation of Methyl Orange. *Catalysis Letters*, **148** (12), 3701-3714.
- Shen T., Wang J., Xia Z., Dai X., Li B. and Feng Y. (2020). Ultraviolet sensing characteristics of Ag-doped ZnO micro-nano fiber. *Sensors and Actuators A Physical*, **307**,1-8. DOI: 10.1016/j.sna.2020.111989
- Shokoochi R., Khazaei M., Godini K., Azarian G., Latifi Z., Javademanesh L. and Nasab H.Z. (2021). Degradation and mineralization of methylene blue dye by peroxymonosulphate/ Mn₃O₄ nanoparticles using central composite design: Kinetic study. *Inorganic Chemistry Communications*, **127**, 108501.
- Subha S.A., El-Subruiti G.M. and Eltaweil A.S. (2018). Facile Synthesis of Ag-γ-Fe₂O₃ Superior Nanocomposite for Catalytic Reduction of Nitroaromatic Compounds and Catalytic Degradation of Methyl Orange. *Catalysis Letters*, **148**(12), 3701-3714. DOI:10.1007/s10562-018-2569-z
- Sumi M.B., Devadiga A., Shetty V. and Saidutta M.B. (2016). Solar photocatalytically active, engineered silver nanoparticle synthesis using aqueous extract of mesocarp of *Cocos nucifera* (Red Spicata Dwarf). *Journal of Experimental Nanoscience*, 1-19. DOI:10.1080/17458080.2016.1251622.
- Uma K., Chen S., Arjun N., Pan G. and Yang T.C.K. (2018). The production of an efficient visible light photocatalyst for CO oxidation through the surface plasmonic resonance effect of Ag nanoparticles on SiO₂@α-Fe₂O₃ nanocomposites. *RCS Advances*, **8**, 12547-12555.
- Wang G., Li F., Li L., Zhao J., Ruan X., Ding W., Cai J., Lu A. and Pei Y. (2020). In Situ Synthesis of Ag-Fe₃O₄ Nanoparticles Immobilized on Pure Cellulose Microspheres as recyclable and biodegradable catalysts. *ACS Omega*, **5**(15), 8839-8846. DOI:10.1021/acsomega.0c00437
- Xu M., Lai C., Liu X., Li B., Zhang M., Xu F., Liu S., Li L., Qin L., Yi H. and Fu Y. (2021). COF-confined catalysts: From nanoparticles and nanoclusters to single atoms. *Journal of Material Chemistry A*, **9** (43), 24148-24174. DOI:10.1039/D1TA04439G
- Zhan S., Li C., Tian H., Ma C., Liu H., Luo J. and Li M. (2019). Synthesis, Characterization and Dye Removal Behavior of Core-Shell-Shell Fe₃O₄/ Ag/ Polyoxometalates Ternary Nanocomposites. *Nanomaterial*, **9** (9), 1255 DOI:10.3390/nano9091255
- Zhang S., Ren F., Wu W., Zhou J., Sun L., Xiao X. and Jiang C. (2014). Size effects of Ag nanoparticles on plasmon-induced enhancement of photocatalysis of Ag-α-Fe₂O₃ nanocomposites. *Journal of Colloids and Interface Science*, **427**, 29-34. DOI:10.1016/j.jcis.2013.12.012